HHS Public Access

Author manuscript

Neuroscience. Author manuscript; available in PMC 2017 June 02.

Published in final edited form as:

Neuroscience. 2016 June 02; 324: 177–190. doi:10.1016/j.neuroscience.2016.03.010.

Intrinsic Plasticity Induced by Group II Metabotropic Glutamate Receptors via Enhancement of High Threshold K_V Currents in Sound Localizing Neurons

William R. Hamlet[1,2,#] and **Yong Lu**[1,2,*]

[1]Department of Anatomy and Neurobiology, College of Medicine, Northeast Ohio Medical University, Rootstown, OH 44272, USA

[2]School of Biomedical Sciences, Kent State University, Kent, OH 44240, USA

Abstract

Intrinsic plasticity has emerged as an important mechanism regulating neuronal excitability and output under physiological and pathological conditions. Here, we report a novel form of intrinsic plasticity. Using perforated patch clamp recordings, we examined the modulatory effects of group II metabotropic glutamate receptors (mGluR II) on voltage-gated potassium (K_V) currents and the firing properties of neurons in the chicken nucleus laminaris (NL), the first central auditory station where interaural time cues are analyzed for sound localization. We found that activation of mGluR II by synthetic agonists resulted in a selective increase of the high threshold K_V currents. More importantly, synaptically released glutamate (with reuptake blocked) also enhanced the high threshold K_V currents. The enhancement was frequency-coding region dependent, being more pronounced in low frequency neurons compared to middle and high frequency neurons. The intracellular mechanism involved the $G_{\beta\gamma}$ signaling pathway associated with phospholipase C and protein kinase C. The modulation strengthened membrane outward rectification, sharpened action potentials, and improved the ability of NL neurons to follow high frequency inputs. These data suggest that mGluR II provides a feedforward modulatory mechanism that may regulate temporal processing under the condition of heightened synaptic inputs.

Keywords

metabotropic glutamate receptor; voltage-gated potassium channel; nucleus laminaris; neuromodulation

[*]Correspondence to: Yong Lu, Ph.D., Department of Anatomy and Neurobiology, College of Medicine, Northeast Ohio Medical University, Rootstown, OH 44272, USA, Telephone: 330-325-6656, Facsimile: 330-325-5916, ylu@neomed.edu.

[#]Current address of William R. Hamlet: University of Pittsburgh, Departments of Otolaryngology and Neurobiology, Pittsburgh, PA 15261

AUTHOR CONTRIBUTIONS

W.H. and Y.L. conceived the study; W.H. and Y.L. designed research; W.H. performed experiments and analyzed data; W.H. and Y.L. wrote the paper.

Conflict of interest: The authors declare no competing financial interests.

INTRODUCTION

Neuromodulation by G-protein coupled receptors (GPCRs) is an important component of neuronal communication that regulates cellular properties and animal behaviors. Via modulation of ion channels and vesicular release machinery, presynaptic GPCRs regulate neurotransmission and are critically involved in synaptic integration and synaptic plasticity (review in Starke et al., 1989; Wu and Saggau, 1997; Catterall and Few, 2008). Recently, a growing body of research has begun to elaborate on the importance of postsynaptic GPCRs and their role in intrinsic plasticity, a process through which postsynaptic neuronal properties are dynamically regulated in response to sensory stimuli and behavioral training (review in Zhang and Linden, 2003; Brown and Kaczmarek, 2011; Kourrich et al., 2015).

As the predominant excitatory neurotransmitter, glutamate acts on ionotropic receptors as well as on G-protein-coupled metabotropic glutamate receptors (mGluRs). Presynaptic mGluRs, functioning as autoreceptors at glutamatergic synapses, or as heteroreceptors at non-glutamatergic synapses, modulate synaptic transmission and thus influence auditory processing in each and every level of the auditory system (review in Lu, 2014). In timing-coding neurons in the avian auditory brainstem, presynaptic mGluRs induce short- and long-term plasticity of the inhibitory inputs to the cochlear nucleus magnocellularis (NM) (Lu, 2007; Tang et al., 2013). In neurons of the nucleus laminaris (NL) where the sound localization cue interaural time difference (ITD) is first computed by detecting converging glutamatergic inputs from the NM, presynaptic mGluRs have been shown to improve coincidence detection via modulation of both the inhibitory (Tang et al., 2009; Tang and Lu, 2012) and excitatory inputs to NL (Okuda et al., 2013). However, very little is known about whether and how postsynaptic mGluRs modulate the intrinsic properties of these neurons.

One intrinsic postsynaptic property of great interest is voltage-gated potassium (K_V) channels, which are strongly expressed in auditory brainstem timing-coding neurons. The low and high threshold K_V (LTK and HTK) components are critical intrinsic determinants of the generation and repolarization of action potentials (APs) (review in Bean, 2007), and both are particularly important for neurons that encode temporal information of auditory stimuli (Brew and Forsythe, 1995; Wang et al. 1998; review in Trussell, 1999; Johnston et al., 2010). The LTK currents activate at membrane voltages near the resting membrane potential (RMP), suppressing excitability and creating a narrow time window for spike generation (review in Golding, 2012). In contrast, the HTK currents activate at membrane voltages near the peak of an AP, narrowing spike width and fastening membrane repolarization and allowing a cell to fire repetitively at high discharge rates (review in Rudy and McBain, 2001). These currents are largely produced by K_V3-subunit containing channels and are prominent in cells that fire APs at high frequencies in the auditory brainstem, including NL neurons (Parameshwaran et al., 2001; Parameshwaran-Iyer et al., 2003; Lu et al., 2004). Although multiple K^+ conductances, such as Ca^{2+}-activated K^+ channels, K_v4-containing channels, and K_v3-containing channels can contribute significantly to the fast repolarization of neuronal membrane (review in Bean, 2007), in NL neurons, K_v3-containing channels are the primary player in AP repolarization (Gao and Lu, 2008). Here, we examined the modulatory role of mGluRs on postsynaptic K_V currents of NL neurons, with a focus on

group II mGluRs (mGluR II), which have been shown to induce intrinsic plasticity via modulating voltage-gated Ca^{2+} channels (review in Zhang and Linden, 2003), and have well-characterized presynaptic effects on synaptic transmission in the NL (Tang et al., 2009; Tang and Lu, 2012; Okuda et al., 2013). We found that activation of mGluR II either by exogenously applied agonists or by synaptically released glutamate, selectively enhanced the HTK currents in NL neurons and directly influenced their firing properties, leading to an improved ability to follow high frequency inputs.

EXPERIMENTAL PROCEDURES

Slice preparation and in vitro conventional whole-cell recordings (WCR)

Brainstem slices (250–300 μm in thickness) were prepared from chick embryos (E17–E18, either sex) as described previously (Tang et al., 2009). Chickens are precocial animals, with hearing onset (able to detect ambient sound) at embryonic day 16 (E16) (Jones et al., 2006). The development of the chicken auditory system completes *in ovo* (Rubel and Parks 1988), and neuronal properties of auditory brainstem neurons are fairly mature by E18 (Gao and Lu, 2008). Adult-like hearing occurs at hatching (Rubel and Parks, 1988; Manley et al., 1991), and behavioral maturation in hearing responses is acquired in early hatchlings (Gray and Rubel, 1985). Therefore, it is conceivable that the cellular data obtained in late embryos in this study reflect approximately the properties at maturation. The ice-cold artificial cerebrospinal fluid (ACSF) used for dissecting and slicing the brain tissue contained the following (in mM): 250 glycerol, 3 KCl, 1.2 KH_2PO_4, 20 $NaHCO_3$, 3 HEPES, 1.2 $CaCl_2$, 5 $MgCl_2$, and 10 dextrose, pH 7.4, when gassed with 95% O_2 and 5% CO_2. The procedures have been approved by the Institutional Animal Care and Use Committee at Northeast Ohio Medical University, and are in accordance with National Institutes of Health policies on animal use. Slices were incubated at 34–36 °C for approximately 1 h in normal ACSF containing the following (in mM): 130 NaCl, 26 $NaHCO_3$, 3 KCl, 3 $CaCl_2$, 1 $MgCl_2$, 1.25 NaH_2PO_4, and 10 dextrose, pH 7.4. For recording, slices were transferred to a 0.5 mL chamber mounted on an upright BX51 microscope (Olympus) with a 40X water-immersion objective. The chamber was continuously superfused with ACSF (1–2 mL/min) driven by gravity.

Patch pipettes were drawn on an Electrode Puller PP-830 (Narishige) to 1–2 μm tip diameter using borosilicate glass micropipettes (inner diameter of 0.86 mm; outer diameter of 1.60 mm) (VWR Scientific). Placement of recording electrodes was controlled by a micromanipulator NMM-25 (Narishige). The electrodes had resistances between 2 and 4 MΩ when filled with a solution containing the following (in mM): 105 K-gluconate, 35 KCl, 5 EGTA, 10 HEPES, 1 $MgCl_2$, 4 ATP-Mg, and 0.3 GTP-Na, with pH of 7.2 (adjusted with KOH) and osmolarity between 280 and 290 mOsm/L. The Cl^- concentration (37 mM) in the internal solution approximated the physiological Cl^- concentration in NL neurons (Tang et al., 2009). The liquid junction potential under conventional WCR was 10 mV, and data were corrected accordingly. In voltage clamp WCR, series resistance (R_s) averaged at 6–8 MΩ, and was compensated by 65–75%. Cells were clamped at a membrane potential of −60 mV. All experiments were conducted using an Axopatch 200B amplifier (Molecular Devices). Data were low-pass filtered at 10 kHz and digitized with a Data Acquisition Interface

ITC-18 (InstruTECH) at 50 kHz. Recording protocols were written and run using the acquisition and analysis software AxoGraph X (AxoGraph Scientific).

Establishment of perforated patch clamp recordings (PPCR)

Dialysis of intracellular soluble signaling molecules has been well understood to be a disadvantage of conventional WCR (Horn and Marty, 1988; Neher, 1988; Falke et al., 1989). We performed PPCR, using antibiotics Nystatin (100 μg/mL) or Escin (40 μM) as the perforating substance, in order to preserve the intracellular environment and prevent possible intracellular dialysis of signaling molecules required for mGluR effects. The tip (first 50–100 μm) of the electrode was filled with normal internal solution and then backfilled with the internal solution containing the perforating antibiotic. Internal solutions were discarded after 2 hrs due to decay of perforating substance. Under PPCR, cells were clamped at a membrane potential of −50 mV, without correction of junction potential, due to the complication in the development and calculation of junction potential under perforated patch configuration (Horn and Marty, 1988; Kim and Trussell, 2007). In fact, Kim and Trussell (2007) found that in gramacidin perforated recordings, the junction potential was likely negligible (approximately 1.4 mV in their study). In our voltage clamp PPCR experiments, series resistance (R_S) averaged at 34.3 MΩ, and was compensated by 60–70%. We did not perform a correction for the uncompensated R_s. The high R_s is one intrinsic limitation of perforated patch recordings. Correction for the uncompensated R_s would result in different V_m under different conditions (e.g. control versus drug application); this would make the comparison of current amplitude at the same V_m impractical.

Given the nature of voltage clamp and space clamp errors in neurons with dendrites (Häusser, 2003; Poleg-Polsky and Diamond, 2011), particularly in recording modes with inevitable high R_S, such as perforated patch clamp (Rall and Segev, 1985; Bar-Yehuda and Korngreen, 2008), establishment of a consistent and reliable PPCR configuration is critical for comparisons of current measurements before and after an experimental manipulation (e.g., drug application or electrical stimulation of presynaptic terminals). Maintenance of PPCR without break-in into conventional WCR ensures that the composition of the cytosol is intact (Chung and Schlichter, 1993; Yawo and Chuhma, 1993; Strauss et al., 2001). Several steps were taken to obtain and maintain PPCR. First, we carefully monitored the uncompensated current responses to a −5 mV test pulse. A gradual decrease in access resistance (R_a) indicated possible successful perforation, while a sudden reduction in R_a indicated WCR mode. Second, we included a non-membrane permeable dye Lucifer Yellow (5 mM) in the recording electrodes. When the membrane ruptured during recording, the dye would be visible inside the neuron (Fig. 1A). In this case, the data was discarded. Finally, the K_V currents recorded in ACSF showed no differences compared to the K_V currents recorded after bath application of a cocktail of drugs to block Na_V channels, hyperpolarization-activated cyclic nucleotide-gated channels (which mediate the I_h current), AMPA receptors, and $GABA_A$ receptors, with tetrodotoxin (TTX, 1 μM), 4-Ethylphenylamino-1,2-dimethyl-6-methylaminopyrimidinium chloride (ZD7288, 80 μM), 6,7-Dinitroquinoxaline-2,3-dione (DNQX, 50 μM), and 6-Imino-3-(4-methoxyphenyl)-1(6*H*)-pyridazinebutanoic acid hydrobromide (gabazine, 20 μM). This indicated that time- and voltage-dependent changes in membrane conductance, if any, under

the PPCR configuration, did not alter the K_V currents of interest (Fig. 1B, n = 8). Therefore, in the subsequent PPCR experiments, the cocktail of blockers (TTX, ZD7288, DNQX, and gabazine) was applied.

Recordings were performed at room temperature (23–25 °C). Although it was preferable to perform the experiments under physiological temperature, we found that it was very difficult to obtain stable long-lasting PPCR at high temperature. Indeed, performing PPCR under room temperature is not an uncommon practice in similar studies (Shirasaki et al., 1994; Song et al., 2005; Leao et al., 2010). Consistently, conventional WCR experiments were also performed at room temperature.

All chemicals were purchased from Sigma-Aldrich except for ZD7288 and gabazine, which were obtained from Tocris, DNQX, 3′,4′,5′,6′-Tetrahydroxyspiro[isobenzofuran-1(3*H*),9′-(9*H*)xanthen]-3-one (Gallein), 3-[1-[3-(Dimethylamino)propyl]-5-methoxy-1*H*-indol-3-yl]-4-(1*H*-indol-3-yl)-1*H*-pyrrole-2,5-dione (Go6983), and 1-[6-[[(17β)-3-Methoxyestra-1,3,5(10)-trien-17-yl]amino]hexyl]-1*H*-pyrrole-2,5-dione (U73122), which were obtained from Abcam, and Lucifer Yellow-Li salt, which was obtained from Biotium.

Identification of tonotopic characteristic frequency (CF) regions

Due to dramatic tonotopic differences of various intrinsic properties of neurons in the NL (Wang et al., 2010), we identified the CF region from which each neuron was recorded. However, it is not possible to precisely define the CF of NL neurons in an *in vitro* slice preparation. Therefore, to categorize neurons into low-, middle-, and high-frequency (LF, MF, and HF) regions, we adapted an approach modified from Kuba et al. (2005), by using the rostral-caudal and medial-lateral position as an indicator of CF. Generally, 5 slices of brainstem tissue containing relevant nuclei were collected, where slice #1 was most caudal and slice #5 was most rostral. Neurons in the lateral NL of slices #2 and #3 were considered LF neurons. MF neurons were considered to be present in the medial NL of slice #2 and #3 and the lateral portion of slice #4. HF neurons were found in the medial portion of slice #4 and in entire slice #5 (Hamlet et al., 2014). MF and HF regions were also confirmed by the presence of a monolayer of NL neurons (Rubel and Parks, 1975). Because boundaries between the regions are subjective, we recorded from neurons clearly present in one of the three CF regions.

Data processing and analysis

For K_v current analysis, leak subtraction was implemented offline using a linear regression to negative voltage steps (−80 to −65 mV) for all the experiments where I_h channels were blocked. The presence of I_h created nonlinearities in the current measurement around RMP, making linear regression-based leak subtraction difficult. Therefore, in one set of experiments (Fig. 3) where I_h was not blocked, leak subtraction was not performed. The RMP was constantly monitored during experiments. The input resistance (R_{in}) was calculated from the voltage responses to a somatic current injection (−50 pA), using Ohm's Law. Current activation was measured by a single exponential function in which A stands for current amplitude, t for time and τ for time constant.

$$f(t)=\mathrm{A} * e^{(-t/\tau)}$$

Data were processed using custom written script for MATLAB (v13, MathWorks), analyzed using PASW (v18, SPSS), and plotted using Igor Pro (v6.01, Wavemetrics). Mean and SEM were reported. Correlations were determined using Pearson's regression analysis. Statistical differences were determined by either paired t-tests, one way Analysis of Variance (ANOVA), or repeated measures Analysis of Variance (RM-ANOVA), using a Greenhouse-Geisser correction. When significant differences were observed in an ANOVA a Tukey's HSD post hoc analysis was conducted to elucidate individual group differences, and when significant differences were observed in an RM-ANOVA, a Bonferroni-corrected paired-comparison was conducted for individual sample comparisons.

RESULTS

PPCR uncovers K_V modulation by mGluR II

After establishing stable perforated recordings (Fig. 1A, B), we sought to examine the effects of mGluR II activation on K_V currents in NL neurons. A robust increase in K_V currents was observed following bath application of DCG-IV (2 μM), a selective mGluR II agonist, in NL neurons across all CF regions in PPCR (n = 16) but not in conventional WCR (n = 8) configuration (Fig. 1C, D). The DCG IV-sensitive K_V current activated at relatively positive voltage commands (about −30 mV), with little to no currents at voltage commands close to RMP (about −60 mV for NL neurons; Fig. 1D *inset*). This strongly suggests that DCG-IV caused an increase primarily in HTK currents.

The detection of mGluR-mediated modulation of K_V currents under PPCR but not WCR may be interpreted by either of the two following scenarios. First, the relatively high R_S and R_a during PPCR might have led to voltage- and space-clamp errors that changed over the course of our recordings. To confidently exclude this possibility, we compared R_{in} and R_S between control and DCG-IV conditions, because changes in R_{in} and R_S can indicate changes in R_a, which was expected to be stable throughout the duration of PPCR. We observed stable R_S (ctr: 34.3 ± 2.2 MΩ, DCG-IV: 34.1 ± 2.1 MΩ, p =0.73) and R_{in} (ctr: 86.4 ± 7.6 MΩ, DCG-IV: 83.4 ± 9.9 MΩ, p = 0.34) across recordings before and after DCG-IV application (Fig. 1E, n = 16). To ensure the stability of R_S during PPCR, we continuously monitored the current responses to a test pulse (−5 mV) in voltage clamp mode. Cells with a change exceeding 15% in the decay time constant (τ_M) of the test-pulse evoked current before and after DCG-IV were discarded. More importantly, we found no correlation between changes in τ_M and changes in K_V currents (Fig. 1F; n = 16, r = 0.047, p = 0.862). This indicates that within the accepted level (<15%) for alteration in R_S, the modulation of K_V was not attributed to voltage- or space-clamp errors due to changes in R_a. Therefore, we considered the second scenario, where one or multiple critical signaling molecules required for the second messenger system is washed out during WCR (Trussell and Jackson, 1987; Horn and Marty, 1988; Vargas et al., 1999). Supporting this notion, perforated but not conventional WCR disclosed mGluR-mediated modulation of other K^+ currents (Shirasaki et al., 1994; Takeshita et al., 1996; Katayama et al., 2003). Therefore, it is likely that under our

WCR configuration dialysis of one or more important components for mGluR II intracellular signaling pathway occurred, resulting in the observation of no modulation of K_V currents.

mGluR II enhancement of K_V currents is most prominent in LF neurons

There is a tonotopic distribution of mGluR II in NL, with LF neurons having as much as a 5-fold higher intensity of immunohistochemistry staining compared to MF and HF neurons (Okuda et al., 2013). We observed similar K_V current density as well as similar modulation by mGluR II in MF and HF neurons, so we compared the amount of mGluR II-enhancement of K_V currents between LF neurons and MF/HF neurons (Fig. 2). We observed increased K_V currents following DCG-IV application in 16 out of 17 neurons (LF, n = 9 of 9; MF and HF, n = 7 of 8). A predominantly high threshold current was enhanced by DCG-IV (Fig. 2A–D). Specifically, in LF neurons, a significant increase in K_V currents was observed at $V_{command}$ of −5 mV (ctr: 0.58 ± 0.12 nA, DCG-IV: 1.72 ± 0.22 nA, $p = 0.002$) and +5 mV (ctr: 1.67 ± 0.24 nA, DCG-IV: 3.95 ± 0.28 nA, $p < 0.001$), but not at −30 mV (ctr: 0.13 ± 0.05 nA, DCG-IV: 0.24 ± 0.08 nA, $p = 0.53$; Fig. 2B). A similar but less dramatic enhancement of K_V currents was observed in MF and HF neurons. There was a significant increase in K_V currents at $V_{command}$ of −5 mV (ctr: 2.21 ± 0.34 nA, DCG-IV: 2.75 ± 0.37 nA, $p = 0.034$) and +5 mV (ctr: 3.04 ± 0.50 nA, DCG-IV: 3.78 ± 0.58 nA, $p = 0.009$), while no significant differences were observed at −30 mV (ctr: 0.50 ± 0.19 nA, DCG-IV: 0.69 ± 0.20 nA, $p = 0.80$; Fig. 2C, D).

To examine the properties of the DCG-IV-sensitive K_V current, we subtracted the K_V currents recorded before DCG-IV from the K_V currents recorded after DCG-IV application in LF neurons (Fig. 2E). Similar to a delayed rectifier conductance, the DCG-IV-sensitive current had slow kinetics, as shown by a large activation τ (16.3 ± 6.3 ms, n = 7) calculated from the currents activated at −5 mV (Fig. 2F). It should be noted that the speed of activation as well as the amplitude of the mGluR-sensitive current would likely be increased under physiological temperatures (Kiernan et al., 2001; Cao and Oertel, 2005). To assess to what extent this modulation varied across the tonotopic axis, we compared the mGluR-enhancement of K_V currents in LF neurons to the K_V enhancement in MF/HF neurons. Comparison of the percent change in K_V currents revealed that there was a significantly larger increase after DCG-IV application in LF compared to MF/HF neurons at −5 mV (LF: 64.0 ± 14.7%, MF/HF: 14.4 ± 6.7%, $p = 0.014$) and +5 mV (LF: 82.7 ± 14.9%, MF: 17.7 ± 7.8%, $p = 0.003$) but not at −30 mV (LF: 14.9 ± 13.6%, MF/HF: 6.7 ± 8.6%, $p = 0.77$; Fig. 2G). These data show that mGluR-enhancement of HTK currents is most prominent in the LF region.

Endogenous glutamate enhances K_V currents in NL neurons

The enhancement of K_V currents by activation of mGluR II is interesting, but it is more important to know whether the modulation is physiologically relevant. To address this issue, we electrically activated the glutamatergic input to NL from the contralateral NM by a bipolar tungsten electrode placed at the midline of the slice where the contralateral NM fibers travel, and examined the effects of synaptic activation on K_V currents in LF neurons under PPCR (Fig. 3A). mGluR II tends to be located distally from glutamate release sites in a large variety of neurons (Tamaru et al., 2001), such as the hippocampus (Shigemoto et al.,

1997), spinal cord (Tang and Sim, 1999), and cerebellar cortex (Ohishi et al., 1994), indicating that these receptors are expressed extrasynaptically. Furthermore, work from our lab has demonstrated that activation of mGluR II by endogenous glutamate in the NL in brain slice preparations is facilitated by blocking glutamate reuptake (Tang et al., 2009), suggesting that mGluR II are located distal from the active zone, thus being active when glutamate spillover occurs. Therefore, we bath applied TFB-TBOA (1 μM), a blocker of astrocyte glutamate reuptake, to reduce potential washout of synaptically released glutamate during ACSF superfusion and to enhance the likelihood of detecting any effect the released glutamate may have on K_V currents. Gabazine (20 μM) was applied to block inhibitory conductances.

Once we confirmed that stimulation of the contralateral fibers produced stable EPSCs in the recorded neuron, we obtained voltage-gated ion channel currents under control and synaptic activation conditions, and measured the steady state K_V current at the end of the voltage step protocol where contamination by Na_V currents was minimal. We did not block Na_V currents because extracellular blockade with TTX would disable synaptic transmission and intracellular blockade with QX314 may also affect K_V currents. We did not block I_h currents in this experiment because it may disrupt the ability of the presynaptic terminal to follow high rates of stimulation. To potentially maximize the release of endogenous glutamate, we applied a train stimulation (500 Hz, 500 pulses, 5 repetitions, 10 s inter-stimulation interval), to the contralateral NM fibers (Fig. 3B). K_V currents were recorded immediately after the stimulation, and again 5 mins later. Immediately after the stimulation we observed a significant increase in steady state K_V currents, and the currents recovered to baseline 5 mins later (Fig. 3C, D, n = 10). There was a significant difference in K_V currents before, immediately after stimulation, and 5 mins after stimulation at −5 mV (ctr: 0.752 ± 0.073 nA; stimulation: 0.873 ± 0.090 nA; recovery: 0.780 ± 0.085 nA; $p = 0.003$) and at +5 mV (ctr: 1.124 ± 0.104 nA; stimulation: 1.358 ± 0.132 nA; recovery: 1.164 ± 0.119 nA, $p < 0.001$) but not at −30 mV (ctr: 0.142 ± 0.023 nA; stimulation: 0.150 ± 0.024 nA; recovery: 0.151 ± 0.022 nA, $p = 0.07$). Bonferroni-corrected pairwise comparisons revealed that there was a significant increase in K_V at −5 mV and +5 mV ($p = 0.006$, $p = 0.001$, respectively) after stimulation and recovery of K_V currents at both holding potentials ($p = 0.05$, $p = 0.003$, respectively) approximately 5 mins after stimulation (Fig. 3E). These data demonstrate that endogenously released glutamate (with reuptake blocked) is sufficient to enhance steady state K_V currents. Moreover, the increased K_V current is similar to that observed by pharmacological mGluR II activation in that the enhancement was most pronounced for the HTK currents. However, the results did not provide direct evidence supporting the involvement of mGluR II in modulation of K_v currents under physiological condition. Experiments using antagonist selective for mGluR II turned out to be difficult because of the small enhancement of K_v currents by synaptically released glutamate. Therefore, we tested the effect of mGluR II antagonist in the next set of experiments in which bath application of drugs was used.

Signaling molecules involved in mGluR II enhancement of K_V currents

To further support the hypothesis that activation of mGluR II was responsible for the increase in HTK currents, we applied an mGluR II selective antagonist, LY341495 (1 μM),

prior to application of DCG-IV. LY341495 eliminated the enhancement of K_V currents by DCG-IV (Fig. 4A, n = 4), with unchanged K_V currents at $V_{command}$ of −30 mV (ctr: 0.26 ± 0.04 nA, DCG-IV: 0.27 ± 0.05 nA, $p = 0.77$), −5 mV (ctr: 1.00 ± 0.22 nA, DCG-IV: 1.03 ± 0.23 nA, $p = 0.53$), and +5 mV (ctr: 1.47 ± 0.41 nA, DCG-IV: 1.39 ± 0.34 nA, $p = 0.06$) (Fig. 4B). GPCRs can modulate intrinsic currents via the G_α subunit or $G_{\beta\gamma}$ complex (review in Hille, 1994; Dascal, 2001). Application of the cell permeable $G_{\beta\gamma}$ blocker gallein (5 μM) to brain slices for 30 mins is sufficient to block $G_{\beta\gamma}$ complex activation (Lehmann et al., 2008; Belkouch et al., 2011; Seneviratne et al., 2011). Therefore, we incubated slices in gallein (5 μM) for >30 mins prior to recording K_V currents. No changes in K_V currents were observed after DCG-IV application in the presence of gallein (Fig. 4C, D, n = 4), at $V_{command}$ of −30 mV (ctr: 0.40 ± 0.13 nA, DCG-IV: 0.46 ± 0.19 nA, $p = 0.54$), −5 mV (ctr: 2.48 ± 0.79 nA, DCG-IV: 2.68 ± 0.97 nA, $p = 0.44$), and +5 mV (ctr: 3.59 ± 1.15 nA, DCG-IV: 3.47 ± 1.12 nA, $p = 0.38$).

The $G_{\beta\gamma}$ complex can activate various signaling pathways including phospholipase C (PLC) (review in Clapham and Neer, 1997; Smrcka, 2008). Therefore, we investigated whether PLC activity was involved in the mGluR-enhancement of K_V currents by incubating slices in cell permeable PLC blocker U73122 (10 μM), 10 mins before and during DCG-IV application. When DCG-IV was applied in the presence of U73122, there was no significant change in K_V currents (Fig. 4E, F; n = 7) at −30 mV (ctr: 0.36 ± 0.07 nA, DCG-IV: 0.38 ± 0.07 nA, $p = 0.24$), −5 mV (ctr: 0.90 ± 0.10 nA, DCG-IV: 0.93 ± 0.11 nA, $p = 0.10$), or + 5 mV (ctr: 1.17 ± 0.12 nA, DCG-IV: 1.24 ± 0.17 nA, $p = 0.18$), suggesting that the $G_{\beta\gamma}$ complex may activate PLC to enhance HTK currents. One way PLC may influence K_V currents is via protein kinase C (PKC) because PLC is known to modulate PKC activity via degradation of phosphatidylinositol 4,5-bisphosphate into diacyl glycerol and inositol 1,4,5-trisphosphate. Previous work on K_V modulation in the mammalian sound localization circuit, as well as in many other brain regions, has shown that PKC can modulate HTK currents (Atzori et al., 2000; Sun et al., 2003), including HTK currents mediated by $K_V3.1$ channels (Critz et al., 1993; Liu and Kaczmarek, 1998; Macica et al., 2003; Song et al., 2005; Song and Kaczmarek, 2006). To test whether PKC was involved, slices were pre-incubated for at least 30 mins in a cell permeable PKC blocker Go6983 (20 nM), which non-selectively blocks all PKC subunits with the exception of PKC_μ (Gschwendt et al., 1996; Peterman et al., 2004). Application of Go6983 before and during DCG-IV exposure prevented K_V modulation (Fig. 4G, H, n = 7), with no significant changes observed at $V_{command}$ of −30 mV (ctr: 0.37 ± 0.08 nA, DCG-IV: 0.36 ± 0.10 nA, $p = 0.86$), −5 mV (ctr: 1.05 ± 0.17 nA, DCG-IV: 1.01 ± 0.13 nA, $p = 0.39$), or +5 mV (ctr: 1.42 ± 0.23 nA, DCG-IV: 1.37 ± 0.16 nA, $p = 0.56$). These results suggest that mGluR II enhancement of K_V currents requires the $G_{\beta\gamma}$ complex pathway associated with PLC and PKC.

mGluR II affects the firing properties of LF neurons

To address the functional relevance of the mGluR II-enhanced K_V current, it is critical to determine how the increased K_V currents modulate the output of NL neurons. Because mGluR II most prominently modulated K_V currents in LF neurons, we examined the effects of mGluR II on voltage deflections and APs in response to current injections in LF neurons. Under current clamp in PPCR, we injected somatic currents using a prolonged pulse

protocol (100 ms pulse duration, $I_{injection}$ = −0.10 to + 0.40 nA) to evoke subthreshold as well as suprathreshold voltage responses. DCG-IV (2 μM) resulted in little to no changes in the RMP (ctr: −56.2 ± 1.2 mV, DCG-IV: −55.5 ± 1.1 mV, p = 0.30, n = 16) (Fig. 5A). However, we revealed subtle but significant reductions in the outward rectification (the ratio of the slope of voltage deflections to depolarized current injections divided by the slope of voltage deflections to hyperpolarized current injections) (ctr: 0.41 ± 0.05, DCG-IV: 0.32 ± 0.04, p = 0.040), reflecting a reduction in membrane voltage in response to the positive current injections (Fig. 5B). In line with an increase in HTK currents, the absolute maximum rate of fall of APs was significantly increased (ctr: −116.2 ± 8.5 mV/ms, DCG-IV: −133.8 ± 9.7 mV/ms, p = 0.017; Fig. 5C), without changing the maximum rate of rise (ctr: 162.9 ± 18.4 mV/ms; DCG-IV: 171.4 ± 21.4 mV/ms, p = 0.07). Spike threshold remained unchanged, in either $I_{threshold}$ (ctr: 0.196 ± 0.034 nA, DCG-IV: 0.201 ± 0.033 nA, p = 0.55) or in $V_{threshold}$ (ctr: 26.9 ± 2.1 mV, DCG-IV: 27.0 ± 1.9 mV, p = 0.34) in response to prolonged current pulses. To further explore whether DCG-IV changed neuronal excitability, we examined the variability in $I_{threshold}$ (rheobase) to short pulse current injections (2 ms of duration, $I_{injection}$ = +0.20 to +0.45 nA). No differences in the rheobase were observed after DCG-IV application (ctr: 0.357 ± 0.038 nA, DCG-IV: 0.347 ± 0.043 nA, p = 0.76, n = 6; data not shown). To examine how DCG-IV modulates individual APs, the AP height and half width at threshold and at I = 0.25 nA were analyzed (Fig. 5D). No change in AP height (measured from RMP) was observed (at threshold, ctr: 91.9 ± 4.5 mV, DCG-IV: 94.9 ± 4.2 mV, p = 0.10; at 0.25 nA, ctr: 102.1 ± 4.6 mV, DCG-IV: 102.0 ± 5.0 mV, p = 0.77; Fig. 5E), while DCG-IV caused a significant reduction in spike half width at 0.25 nA (ctr: 1.15 ± 0.08 ms, DCG-IV: 1.09 ± 0.09 ms, p = 0.010) but not at threshold (ctr: 1.13 ± 0.08 ms, DCG-IV: 1.18 ± 0.13 ms, p = 0.38; Fig. 5F). In summary, DCG-IV produced subtle but significant changes in membrane rectification, AP rate of fall, and AP half width of NL neurons, without affecting RMP, AP rate of rise, or spike threshold. These results are consistent with the selective enhancement of HTK but not LTK currents by mGluR II in NL neurons.

mGluR II enhances the high frequency following ability of LF neurons

The enhancement of HTK currents by mGluRs presents a feedforward modulatory mechanism to dynamically regulate the output of neurons, particularly when the neurons are undergoing periods of high activity. One major role of HTK currents is to maintain high frequency firing by allowing a neuron to repolarize rapidly, thus producing narrow APs (review in Rudy et al., 1999; Rudy and McBain, 2001; Johnston et al., 2010). Therefore, we predicted that enhancement of K_V currents by mGluR II in NL neurons would enable them to fire at higher rates due to increased rate of membrane repolarization and reduced AP width. To test this hypothesis, we injected trains of 50, 100, and 200 Hz square current pulses (1 ms pulses, 500 ms train stimulation duration) to the recorded cells and examined the effects of DCG-IV (2 μM) (Fig. 6A). Synaptic activation was not used to evoke spike activity, because presynaptic mGluRs including mGluR II suppress glutamatergic transmission especially in low frequency NL neurons (Okuda et al., 2013), in which we observed the strongest mGluR II modulatory effect on K_V currents. Therefore, to evoke spike activity using synaptic activation would complicate the interpretation. Current injections avoided such complications. The amplitude of the current pulses was set to 10 times the current threshold measured with the long pulse current protocol. Because the HTK

currents were increased during DCG-IV application, the relatively slowly activating HTK currents should progressively decrease AP peaks during high frequency current injections. Indeed, when we compared the height of the first and last AP evoked by the same train stimulation protocol, we found that DCG-IV decreased AP height significantly at all frequencies tested (Fig. 6B–D, *left panels*): 50 Hz (ctr: −3.7 ± 4.1%, DCG-IV: −12.1 ± 3.0%, $p = 0.012$), 100 Hz (ctr: −10.2 ± 4.4%, DCG-IV: −22.4 ± 2.6%, $p = 0.005$), and 200 Hz (ctr: −22.8 ± 4.5%, DCG-IV: −36.1 ± 5.7%, $p < 0.001$). Additionally, with increased HTK currents, neurons should fire APs more reliably in response to high frequency somatic current injections. To assess this, we examined the number and rate of failures and the variability of time between spikes. DCG-IV significantly decreased the percent of failures (i.e., increased success rate for firing) at all frequencies tested (Fig. 6B–D, *middle left*): 50 Hz (ctr: 42.8 ± 10.0%, DCG-IV: 32.3 ± 9.8%, $p = 0.013$), 100 Hz (ctr: 41.4 ± 6.1%, DCG-IV: 26.8 ± 5.7%, $p = 0.004$), and 200 Hz (ctr: 65.8 ± 7.7%, DCG-IV: 53.5 ± 7.3%, $p = 0.0228$). Thus mGluR II activation increased the number of APs to all test frequencies (Fig. 6B–D, *middle right*): 50 Hz (ctr: 14.3 ± 2.5, DCG-IV: 16.9 ± 2.5, $p = 0.013$), 100 Hz (ctr: 29.2 ± 3.1, DCG-IV: 37.1 ± 2.8, $p = 0.004$), and 200 Hz (ctr: 34.2 ± 7.7, DCG-IV: 46.5 ± 7.3, $p = 0.023$). DCG-IV also significantly reduced the coefficient of variation of inter-spike interval (ISI CV) during train stimulation at 50 Hz (ctr: 0.051 ± 0.020, DCG-IV: 0.030 ± 0.015, $p = 0.004$) and 100 Hz (ctr: 0.061 ± 0.012, DCG-IV: 0.043 ± 0.009, $p = 0.013$). A small but consistent reduction in ISI CV at 200 Hz was observed (ctr: 0.146 ± 0.071, DCG-IV: 0.062 ± 0.034, $p = 0.057$) (Fig. 6B–D, *right panels*). Together, these data further confirm the observation under voltage clamp that DCG-IV increases the HTK current in NL neurons. The increased HTK current decreased AP height during the course of somatic train stimulation and increased the reliability of an NL neuron to follow high frequency stimulation. It is worth noting that the experiments in our study were done under room temperature. At physiological temperature, repolarization of APs will be accelerated due to faster activation of K_V channels. The role of mGluR-enhanced K_V conductance might not be as prominent as at room temperature.

DISCUSSION

The results of this study reveal that mGluR II enhances the HTK currents in NL neurons, providing a novel feedforward modulatory mechanism regulating postsynaptic neuronal properties in the sound localization circuit. This modulation is most prominent in LF neurons, in which the baseline K_V currents are relatively weaker while the expression of mGluR II is stronger compared to MF/HF neurons. The modulation is dependent on activity of the $G_{\beta\gamma}$ complex, PLC, and PKC. The enhancement of the HTK currents improves NL neurons' ability to follow high frequency inputs. Our discussion below focuses on the tonotopic nature of this modulation, the signaling pathway, and the functional implications.

The HTK but not the LTK component is subject to mGluR II modulation. Several lines of evidence lead us to believe this observation is unlikely the result of voltage clamp errors. Due to relatively high R_S (34.3 ± 2.2 MΩ) in PPCR in addition to the presence of extensive dendrites in LF neurons, space clamp and voltage clamp errors may have arisen (Häusser, 2003; Bar-Yehuda and Korngreen, 2008), leading to possible ambiguous determination of activation voltages for LTK versus HTK currents. However, the LTK currents are strongly

active near RMP in NL neurons (Hamlet et al., 2014), and are readily activated by small membrane depolarizations. At $V_{command}$ of −30 mV, the LTK currents were expected to be highly active, and no mGluR II modulation was observed. At −5 and +5 mV, the HTK currents were active, and mGluR II enhancement of the currents was significant (Fig. 2), clearly indicating that the modulation was selective for the HTK component. The conclusion that mGluR II enhancement of K_V currents is selective for the HTK component is further supported by our current clamp recordings. Activation of mGluR II did not change the neuronal properties (e.g., RMP, $I_{threshold}$, $V_{threshold}$, and rheobase) that are regulated by the LTK currents. In contrast, the neuronal properties that are regulated by the HTK currents (e.g., membrane outward rectification, AP rate of fall, AP width, and high frequency following ability) were significantly altered. Therefore, despite the limitations of voltage control in voltage clamp recordings under PPCR configuration, our data strongly suggest that the HTK channels are the primary modulatory targets of mGluR II in NL neurons.

Our results revealed a tonotopic distribution of mGluR II modulation of K_V currents in NL neurons. The protein expression of mGluR II is the strongest in LF region (Okuda et al., 2013), where the enhancement by mGluR II is the most prominent, resulting in a highly dynamic HTK current. Such a dynamic HTK current in LF neurons was also reported for the mammalian medial nucleus of the trapezoid body (MNTB), a critical nucleus involved in the sound localization circuit. In MNTB, while there is no gradient in the protein expression of mGluR II (Elezgarai et al., 2001), somatic $K_V3.1$ channels are tonotopically arranged, with LF neurons having weaker K_V currents than HF neurons (Wang et al., 1998; Li et al., 2001; Brew and Forsythe, 2005; Leão et al., 2006). Interestingly, sound or electrical activation of afferent fibers to MNTB induces an increase in HTK currents, and the increase is larger in LF neurons (Leão et al., 2010), suggesting that the HTK currents in LF neurons are more dynamical (Song et al., 2005; Leão et al., 2010). Why would LF NL neurons require highly dynamic HTK currents? A plausible interpretation may reside in the patterns of their synaptic inputs. MF and HF neurons may possess higher spontaneous synaptic activity than LF neurons (Nishino et al., 2008). Thus, at rest (a “quiet” state) LF neurons receive fewer synaptic inputs, and mGluR II activity is presumably low. During sound stimulation (an “active” state), LF neurons receive strong excitatory inputs from NM (Nishino et al., 2008). Therefore, a mechanism may be present to allow LF neurons to adapt to the dramatic change in the amount of synaptic inputs. In contrast, MF and HF neurons constantly receive relatively more numerous and stronger synaptic inputs, even at rest (Kuba et al., 2005; Nishino et al., 2008; Sanchez et al., 2010; Hamlet et al., 2014), reducing the need for such a dynamic HTK current for regulation of spiking activity. These data are in line with the idea that the tonotopic distribution of synaptic inputs may be complemented by tonotopic distribution of mGluR modulation for auditory processing (review in Lu, 2014).

mGluR II can cause intracellular changes through the G_α, $G_{\beta\gamma}$ complex, or a combination of both (review in Niswender and Conn, 2010; Nicoletti et al., 2011). We show that blocking the $G_{\beta\gamma}$ complex prevented the DCG-IV enhancement of K_V currents in NL neurons, indicating signaling transduction via the $G_{\beta\gamma}$ complex. Downstream to the $G_{\beta\gamma}$ complex is the activation of PLC, followed by the cleavage of phosphatidylinositol 4,5-bisphosphate into diacyl glycerol and inositol 1,4,5-trisphosphate, which can change the activity of PKC (review in Clapham and Neer, 1997; Smrcka, 2008). Our data support that PLC and PKC are

critical factors for the modulation of K_V currents by mGluR II in NL. There is a large body of literature showing how the HTK channels can be modulated by the phosphorylation state of specific subunits (e.g. Augustine and Bezanilla, 1990; Atzori et al., 2000; Strumbos et al., 2010). Much of the literature concerning phosphorylation-induced changes in K_V3 currents has shown that PKC is intimately involved (Liu and Kaczmarek, 1998; Macica et al., 2003; Sun et al., 2003; Song et al., 2005; Song and Kaczmarek, 2006). However, exactly how activation of mGluR II leads to activation of the $G_{\beta\gamma}$ complex, which changes PKC activity via PLC, and ultimately causes an enhancement of HTK currents in NL neurons, awaits more investigation. At the same time, we cannot completely rule out the involvement of G_α in mGluR II enhancement of K_V currents. One important issue to consider is the ability of PKC to inhibit interactions between G_α subunit and adenylate cyclase (Gordeladze et al., 1989; García-Sáinz and Gutiérrez-Venegas, 1989), and the direct reduction of K_V currents due to increased rate of K_V inactivation by cAMP (Chung and Kaczmarek, 1995).

Taken together, our results suggest that via mGluR II the glutamatergic input to the NL can provide a feedforward modulatory mechanism to improve the high frequency following ability of NL neurons. The increased ability to follow high frequency inputs due to enhanced HTK conductance seems to be in contrast with the observation that suppression of HTK conductance enhances the overall excitability and spike generation (Dong et al., 2005). However, enhancement of HTK conductance could increase spike generation through interaction with other ion channels. For example, the enhanced HTK currents may allow faster recovery of Na_V channels from inactivation and promote activation of resurgent Na_V currents (Akemann and Knöpfel., 2006), producing more and faster APs. Importantly, mGluRs reduced the temporal variability of NL spikes, suggesting that NL neurons can dynamically regulate their ability to follow high frequency inputs depending on the history of previous inputs. Song et al. (2005) proposed that in quiet environments neurons have improved temporal precision but a reduced ability to follow high frequency stimulation, while in noisy environments the ability to follow high frequency stimulation is improved at the expense of temporal precision. This allows adaptive ion channel changes in response to altered sensory stimuli (Song et al., 2005; Strumbos et al., 2010). It is not certain whether there would be a loss of temporal fidelity after mGluR II induced K_V enhancement in NL neurons, because altered temporal processing is usually assessed with spike trains evoked by presynaptic inputs but not postsynaptic current injection (Xie and Manis, 2013). It remains to be determined whether the precision of temporal processing is necessarily compromised under high frequency input in NL neurons. Finally, LF neurons have a large dynamic range in their synaptic inputs from the NM, and enhancement of K_V currents may allow these neurons to adapt to the dramatic changes in the strength of inputs from resting to active states, an intrinsic plasticity that may play a role in temporal processing.

Acknowledgments

We thank Calum Grimsley and Dr. Sharad Shanbhag for advice with MATLAB coding, Nichole Foster and Dr. Jeffrey Mellott for imaging of dye-filled neurons, and Rebecca Curry for helpful discussion and comments. This work was supported by National Institute on Deafness and other Communication Disorders Grant R01DC008984 and an Institutional Bridge Funding (Y.L.).

ABBREVIATIONS

ACSF	artificial cerebrospinal fluid
AP	action potential
CF	characteristic frequency
GPCR	G protein-coupled receptor
HF	high frequency
HTK	high-threshold potassium
ITD	interaural time difference
K_V	voltage-gated potassium channel
LF	low frequency
LTK	low-threshold potassium
mGluR	metabotropic glutamate receptor
MF	middle frequency
MNTB	medial nucleus of trapzoid body
Na_V	voltage-gated sodium channel
NM	nucleus magnocellularis
NL	nucleus laminaris
PKC	protein kinase C
PLC	phospholipase C
PPCR	perforated patch clamp recording
RMP	resting membrane potential
WCR	whole-cell recording

References

Akemann W, Knöpfel T. Interaction of K_V3 potassium channels and resurgent sodium current influences the rate of spontaneous firing of Purkinje neurons. J Neurosci. 2006; 26:4602–4612. [PubMed: 16641240]

Atzori M, Lau D, Tansey EP, Chow A, Ozaita A, Rudy B, McBain CJ. H_2 histamine receptor-phosphorylation of $K_V3.2$ modulates interneuron fast spiking. Nat Neurosci. 2000; 3:791–798. [PubMed: 10903572]

Augustine CK, Bezanilla F. Phosphorylation modulates potassium conductance and gating current of perfused giant axons of squid. J Gen Physiol. 1990; 95:245–271. [PubMed: 2307959]

Bar-Yehuda D, Korngreen A. Space-clamp problems when voltage clamping neurons expressing voltage-gated conductances. J Neurophysiol. 2008; 99:1127–1136. [PubMed: 18184885]

Bean BP. The action potential in mammalian central neurons. Nat Rev Neurosci. 2007; 8:451–465. [PubMed: 17514198]

Belkouch M, Dansereau M-A, Réaux-Le Goazigo A, Van Steenwinckel J, Beaudet N, Chraibi A, Melik-Parsadaniantz S, Sarret P. The chemokine CCL2 increases $Na_V1.8$ sodium channel activity in primary sensory neurons through a $G_{\beta\gamma}$-dependent mechanism. J Neurosci. 2011; 31:18381–18390. [PubMed: 22171040]

Brew HM, Forsythe ID. Two voltage-dependent K^+ conductances with complementary functions in postsynaptic integration at a central auditory synapse. J Neurosci. 1995; 15:8011–8022. [PubMed: 8613738]

Brew HM, Forsythe ID. Systematic variation of potassium current amplitudes across the tonotopic axis of the rat medial nucleus of the trapezoid body. Hear Res. 2005; 206:116–132. [PubMed: 16081003]

Brown MR, Kaczmarek LK. Potassium channel modulation and auditory processing. Hear Res. 2011; 279:32–42. [PubMed: 21414395]

Cao XJ, Oertel D. Temperature affects voltage-sensitive conductances differentially in octopus cells of the mammalian cochlear nucleus. J Neurophysiol. 2005; 94:821–832. [PubMed: 15800074]

Catterall WA, Few AP. Calcium channel regulation and presynaptic plasticity. Neuron. 2008; 59:882–901. [PubMed: 18817729]

Chung I, Schlichter LC. Criteria for perforated-patch recordings: ion currents versus dye permeation in human T lymphocytes. Pflugers Arch. 1993; 424:511–515. [PubMed: 8255735]

Chung S, Kaczmarek LK. Modulation of the inactivation of voltage-dependent potassium channels by cAMP. J Neurosci. 1995; 15:3927–3935. [PubMed: 7751955]

Clapham DE, Neer EJ. G protein βγ subunits. Annu Rev Pharmacol Toxicol. 1997; 37:167–203. [PubMed: 9131251]

Critz SD, Wible BA, Lopez HS, Brown AM. Stable expression and regulation of a rat brain K^+ Channel. J Neurochem. 1993; 60:1175–1178. [PubMed: 8436968]

Dascal N. Ion-channel regulation by G proteins. Trends Endocrinol Metab. 2001; 12:391–398. [PubMed: 11595540]

Dong Y, Nasif FJ, Tsui JJ, Ju WY, Cooper DC, Hu X-T, Malenka RC, White FJ. Cocaine-induced plasticity of intrinsic membrane properties in prefrontal cortex pyramidal neurons: adaptations in potassium currents. J Neurosci. 2005; 25:936–940. [PubMed: 15673674]

Elezgarai I, Bilbao A, Mateos JM, Azkue JJ, Benítez R, Osorio A, Díez J, Puente N, Doñate-Oliver F, Grandes P. Group II metabotropic glutamate receptors are differentially expressed in the medial nucleus of the trapezoid body in the developing and adult rat. Neuroscience. 2001; 104:487–498. [PubMed: 11377849]

Falke LC, Gillis KD, Pressel DM, Misler S. 'Perforated patch recording' allows long-term monitoring of metabolite-induced electrical activity and voltage-dependent Ca^{2+} currents in pancreatic islet B cells. FEBS Lett. 1989; 251:167–172. [PubMed: 2473925]

Gao H, Lu Y. Early development of intrinsic and synaptic properties of chicken nucleus laminaris neurons. Neuroscience. 2008; 153:131–143. [PubMed: 18355968]

García-Sáinz JA, Gutiérrez-Venegas G. Activation of protein kinase C alters the interaction of α_2-adrenoceptors and the inhibitory GTP-binding protein (G_i) in human platelets. FEBS Lett. 1989; 257:427–430. [PubMed: 2555224]

Golding, NL. Neuronal response properties and voltage-gated ion channels in the auditory system. In: Trussell, LO.Popper, AN., Fay, RR., editors. Synaptic mechanisms in the auditory system. New York: Springer P; 2012. p. 7-41.

Gordeladze JO, Björo T, Torjesen PA, Ostberg BC, Haug E, Gautvik KM. Protein kinase C stimulates adenylate cyclase activity in prolactin-secreting rat adenoma (GH_4C_1) pituicytes by inactivating the inhibitory GTP-binding protein G_i. Eur J Biochem. 1989; 183:397–406. [PubMed: 2569396]

Gray L, Rubel EW. Development of absolute thresholds in chickens. J Acoust Soc Am. 1985; 77:1162–1172. [PubMed: 3980868]

Gschwendt M, Dieterich S, Rennecke J, Kittstein W, Mueller HJ, Johannes FJ. Inhibition of protein kinase C μ by various inhibitors: Differentiation from protein kinase c isoenzymes. FEBS Lett. 1996; 392:77–80. [PubMed: 8772178]

Hamlet WR, Liu Y-W, Tang Z-Q, Lu Y. Interplay between low threshold voltage-gated K^+ channels and synaptic inhibition in neurons of the chicken nucleus laminaris along its frequency axis. Front Neural Circuits. 2014; 8doi: 10.3389/fncir.2014.00051

Häusser M. Revealing the properties of dendritic voltage-gated channels: a new approach to the space clamp problem. Biophys J. 2003; 84:3497–3498. [PubMed: 12770861]

Hille B. Modulation of ion-channel function by G-protein-coupled receptors. Trends Neurosci. 1994; 17:531–536. [PubMed: 7532338]

Horn R, Marty A. Muscarinic activation of ionic currents measured by a new whole-cell recording method. J Gen Physiol. 1988; 92:145–159. [PubMed: 2459299]

Johnston J, Forsythe ID, Kopp-Scheinpflug C. Going native: voltage-gated potassium channels controlling neuronal excitability. J Physiol (Lond). 2010; 588:3187–3200. [PubMed: 20519310]

Jones TA, Jones SM, Paggett KC. Emergence of Hearing in the Chicken Embryo. J Neurophysiol. 2006; 96(1):128–141. [PubMed: 16598067]

Katayama J, Akaike N, Nabekura J. Characterization of pre- and post-synaptic metabotropic glutamate receptor-mediated inhibitory responses in substantia nigra dopamine neurons. Neurosci Res. 2003; 45:101–115. [PubMed: 12507729]

Kiernan MC, Cikurel K, Bostock H. Effects of temperature on the excitability properties of human motor axons. Brain. 2001; 124:816–825. [PubMed: 11287380]

Kim Y, Trussell LO. Ion channels generating complex spikes in cartwheel cells of the dorsal cochlear nucleus. J Neurophysiol. 2007; 97:1705–1725. [PubMed: 17289937]

Kourrich S, Calu DJ, Bonci A. Intrinsic plasticity: an emerging player in addiction. Nat Rev Neurosci. 2015; 16:173–184. [PubMed: 25697160]

Kuba H, Yamada R, Fukui I, Ohmori H. Tonotopic specialization of auditory coincidence detection in nucleus laminaris of the chick. J Neurosci. 2005; 25:1924–1934. [PubMed: 15728832]

Leão RN, Sun H, Svahn K, Berntson A, Youssoufian M, Paolini AG, Fyffe RE, Walmsley B. Topographic organization in the auditory brainstem of juvenile mice is disrupted in congenital deafness. J Physiol (Lond). 2006; 571:563–578. [PubMed: 16373385]

Leão KE, Leão RN, Deardorff AS, Garrett A, Fyffe R, Walmsley B. Sound stimulation modulates high-threshold K^+ currents in mouse auditory brainstem neurons. Eur J Neurosci. 2010; 32:1658–1667. [PubMed: 20946234]

Lehmann DM, Seneviratne AMPB, Smrcka AV. Small molecule disruption of G protein $\beta\gamma$ subunit signaling inhibits neutrophil chemotaxis and inflammation. Mol Pharmacol. 2008; 73:410–418. [PubMed: 18006643]

Li W, Kaczmarek LK, Perney TM. Localization of two high-threshold potassium channel subunits in the rat central auditory system. J Comp Neurol. 2001; 437:196–218. [PubMed: 11494252]

Liu SJ, Kaczmarek LK. The expression of two splice variants of the $K_V3.1$ potassium channel gene is regulated by different signaling pathways. J Neurosci. 1998; 18:2881–2890. [PubMed: 9526005]

Lu Y, Monsivais P, Tempel BL, Rubel EW. Activity-dependent regulation of the potassium channel subunits Kv1.1 and Kv3.1. J Comp Neurol. 2004; 470:93–106. [PubMed: 14755528]

Lu Y. Endogenous mGluR activity suppresses GABAergic transmission in avian cochlear nucleus magnocellularis neurons. J Neurophysiol. 2007; 97:1018–1029. [PubMed: 17135473]

Lu Y. Metabotropic glutamate receptors in auditory processing. Neuroscience. 2014; 274:429–445. [PubMed: 24909898]

Macica CM, von Hehn CA, Wang LY, Ho CS, Yokoyama S, Joho RH, Kaczmarek LK. Modulation of the $K_V3.1b$ potassium channel isoform adjusts the fidelity of the firing pattern of auditory neurons. J Neurosci. 2003; 23:1133–1141. [PubMed: 12598601]

Manley GA, Kaiser A, Brix J, Gleich O. Activity patterns of primary auditory-nerve fibres in chickens: development of fundamental properties. Hear Res. 1991; 57:1–15. [PubMed: 1774201]

Neher E. The use of the patch clamp technique to study second messenger-mediated cellular events. Neuroscience. 1988; 26:727–734. [PubMed: 2462183]

Nicoletti F, Bockaert J, Collingridge GL, Conn PJ, Ferraguti F, Schoepp DD, Wroblewski JT, Pin JP. Metabotropic glutamate receptors: From the workbench to the bedside. Neuropharmacology. 2011; 60:1017–1041. [PubMed: 21036182]

Nishino E, Yamada R, Kuba H, Hioki H, Furuta T, Kaneko T, Ohmori H. Sound-intensity-dependent compensation for the small interaural time difference cue for sound source localization. J Neurosci. 2008; 28:7153–7164. [PubMed: 18614685]

Niswender CM, Conn PJ. Metabotropic glutamate receptors: physiology, pharmacology, and disease. Annu Rev Pharmacol Toxicol. 2010; 50:295–322. [PubMed: 20055706]

Ohishi H, Ogawa-Meguro R, Shigemoto R, Kaneko T, Nakanishi S, Mizuno N. Immunohistochemical localization of metabotropic glutamate receptors, mGluR2 and mGluR3, in rat cerebellar cortex. Neuron. 1994; 13:55–66. [PubMed: 8043281]

Okuda H, Yamada R, Kuba H, Ohmori H. Activation of metabotropic glutamate receptors improves the accuracy of coincidence detection by presynaptic mechanisms in the nucleus laminaris of the chick. J Physiol (Lond). 2013; 591:365–378. [PubMed: 23090950]

Parameshwaran S, Carr CE, Perney TM. Expression of the Kv3.1 potassium channel in the avian auditory brainstem. J Neurosci. 2001; 21:485–494. [PubMed: 11160428]

Parameshwaran-Iyer S, Carr CE, Perney TM. Localization of KCNC1 (K_V3.1) potassium channel subunits in the avian auditory nucleus magnocellularis and nucleus laminaris during development. J Neurobiol. 2003; 55:165–178. [PubMed: 12672015]

Peterman EE, Taormina P, Harvey M, Young LH. Gö 6983 exerts cardioprotective effects in myocardial ischemia/reperfusion. J Cardiovasc Pharmacol. 2004; 43:645–656. [PubMed: 15071351]

Poleg-Polsky A, Diamond JS. Imperfect space clamp permits electrotonic interactions between inhibitory and excitatory synaptic conductances, distorting voltage clamp recordings. PLOS ONE. 2011; 6:e19463. [PubMed: 21559357]

Rall, W., Segev, I. Space-clamp problems when voltage clamping branched neurons with intracellular microelectrodes. In: Smith, TG.Lecar, H.Redman, SJ., Gage, PW., editors. Voltage and patch clamping with microelectrodes. New York: Springer P; 1985. p. 191-215.

Rubel EW, Parks TN. Organization and development of brain stem auditory nuclei of the chicken: tonotopic organization of n. magnocellularis and n. laminaris. J Comp Neurol. 1975; 164:411–433. [PubMed: 1206127]

Rubel, EW., Parks, TN. Organization and development of the avian brain-stem auditory system. In: Edelman, GM.Einar Gall, W., Maxwell Cowan, W., editors. Brain function. New York: John Wiley & Sons; 1988. p. 3-92.

Rudy B, Chow A, Lau D, Amarillo Y, Ozaita A, Saganich M, Moreno H, Nadal MS, Hernandez-Pineda R, Hernandez-Cruz A, Erisir A, Leonard C, Vega-Saenz de Miera E. Contributions of K_V3 channels to neuronal excitability. Ann N Y Acad Sci. 1999; 868:304–343. [PubMed: 10414303]

Rudy B, McBain CJ. K_V3 channels: voltage-gated K^+ channels designed for high-frequency repetitive firing. Trend Neurosci. 2001; 24:517–526. [PubMed: 11506885]

Sanchez JT, Wang Y, Rubel EW, Barria A. Development of glutamatergic synaptic transmission in binaural auditory neurons. J Neurophysiol. 2010; 104:1774–1789. [PubMed: 20668278]

Seneviratne AM, Burroughs M, Giralt E, Smrcka AV. Direct-reversible binding of small molecules to G protein $\beta\gamma$ subunits. Biochim Biophys Acta. 2011; 1814:1210–1218. [PubMed: 21621014]

Shigemoto R, Kinoshita A, Wada E, Nomura S, Ohishi H, Takada M, Flor PJ, Neki A, Abe T, Nakanishi S, Mizuno N. Differential presynaptic localization of metabotropic glutamate receptor subtypes in the rat hippocampus. J Neurosci. 1997; 17:7503–7522. [PubMed: 9295396]

Shirasaki T, Harata N, Akaike N. Metabotropic glutamate response in acutely dissociated hippocampal CA1 pyramidal neurones of the rat. J Physiol (Lond). 1994; 475:439–453. [PubMed: 7911830]

Smrcka AV. G protein $\beta\gamma$ subunits: central mediators of G protein-coupled receptor signaling. Cell Mol Life Sci. 2008; 65:2191–2214. [PubMed: 18488142]

Song P, Yang Y, Barnes-Davies M, Bhattacharjee A, Hamann M, Forsythe ID, Oliver DL, Kaczmarek LK. Acoustic environment determines phosphorylation state of the K_V3.1 potassium channel in auditory neurons. Nat Neurosci. 2005; 8:1335–1342. [PubMed: 16136041]

Song P, Kaczmarek LK. Modulation of K_V3.1b potassium channel phosphorylation in auditory neurons by conventional and novel protein kinase C isozymes. J Biol Chem. 2006; 281:15582–15591. [PubMed: 16595659]

Starke K, Gothert M, Kilbinger H. Modulation of neurotransmitter release by presynaptic autoreceptors. Physiol Rev. 1989; 69:864–989. [PubMed: 2568648]

Strauss U, Herbrik M, Mix E, Schubert R, Rolfs A. Whole-cell patch-clamp: true perforated or spontaneous conventional recordings? Pflugers Arch. 2001; 442:634–638. [PubMed: 11510897]

Strumbos JG, Polley DB, Kaczmarek LK. Specific and rapid effects of acoustic stimulation on the tonotopic distribution of $K_V3.1b$ potassium channels in the adult rat. Neuroscience. 2010; 167:567–572. [PubMed: 20219640]

Sun C, Du J, Raizada MK, Sumners C. Modulation of delayed rectifier potassium current by angiotensin II in CATH.a cells. Biochem Biophys Res Comm. 2003; 310:710–714. [PubMed: 14550259]

Takeshita Y, Harata N, Akaike N. Suppression of K^+ conductance by metabotropic glutamate receptor in acutely dissociated large cholinergic neurons of rat caudate putamen. J Neurophysiol. 1996; 76:1545–1558. [PubMed: 8890274]

Tamaru Y, Nomura S, Mizuno N, Shigemoto R. Distribution of metabotropic glutamate receptor mGluR3 in the mouse CNS: differential location relative to pre- and postsynaptic sites. Neuroscience. 2001; 106:481–503. [PubMed: 11591452]

Tang FR, Sim MK. Pre- and/or post-synaptic localization of metabotropic glutamate receptor 1α (mGluR1α) and 2/3 (mGluR2/3) in the rat spinal cord. Neurosci Res. 1999; 34:73–78. [PubMed: 10498333]

Tang ZQ, Gao H, Lu Y. Control of a depolarizing GABAergic input in an auditory coincidence detection circuit. J Neurophysiol. 2009; 102:1672–1683. [PubMed: 19571192]

Tang ZQ, Lu Y. Development of GPCR modulation of GABAergic transmission in chicken nucleus laminaris neurons. PLOS ONE. 2012; 7:e35831. [PubMed: 22545142]

Tang ZQ, Liu YW, Shi W, Dinh EH, Hamlet WR, Curry RJ, Lu Y. Activation of synaptic group II metabotropic glutamate receptors induces long-term depression at GABAergic synapses in CNS neurons. J Neurosci. 2013; 33:15964–15977. [PubMed: 24089501]

Trussell LO, Jackson MB. Dependence of an adenosine-activated potassium current on a GTP-binding protein in mammalian central neurons. J Neurosci. 1987; 7:3306–3316. [PubMed: 2822865]

Trussell LO. Synaptic mechanisms for coding timing in auditory neurons. Annu Rev Physiol. 1999; 61:477–496. [PubMed: 10099698]

Vargas G, Yeh TY, Blumenthal DK, Lucero MT. Common components of patch-clamp internal recording solutions can significantly affect protein kinase A activity. Brain Res. 1999; 828:169–173. [PubMed: 10320738]

Wang LY, Gan L, Forsythe ID, Kaczmarek LK. Contribution of the $K_V3.1$ potassium channel to high-frequency firing in mouse auditory neurones. J Physiol (Lond). 1998; 509:183–194. [PubMed: 9547392]

Wang, Y., Sanchez, JT., Rubel, EW. Nucleus laminaris. In: Shepherd, G., Grillner, S., editors. Handbook of brain microcircuits. New York: Oxford UP; 2010. p. 224-234.

Wu LG, Saggau P. Presynaptic inhibition of elicited neurotransmitter release. Trends Neurosci. 1997; 20:204–212. [PubMed: 9141196]

Xie R, Manis PB. Target-specific IPSC kinetics promote temporal processing in auditory parallel pathways. J Neurosci. 2013; 33:1598–1614. [PubMed: 23345233]

Yawo H, Chuhma N. An improved method for perforated patch recordings using nystatin-fluorescein mixture. Jpn J Physiol. 1993; 43:267–273. [PubMed: 8355424]

Zhang W, Linden DJ. The other side of the engram: experience-driven changes in neuronal intrinsic excitability. Nat Rev Neurosci. 2003; 4:885–900. [PubMed: 14595400]

Highlights

- Perforated patch clamp recordings revealed modulation of K_v channel currents in nucleus laminaris neurons
- Group II metabotropic glutamate receptors mediated the modulation via signaling pathway involving PLC and PKC
- The modulation was more pronounced in low frequency than in middle and high frequency neurons
- The modulation improved the ability of nucleus laminaris neurons to follow high frequency inputs

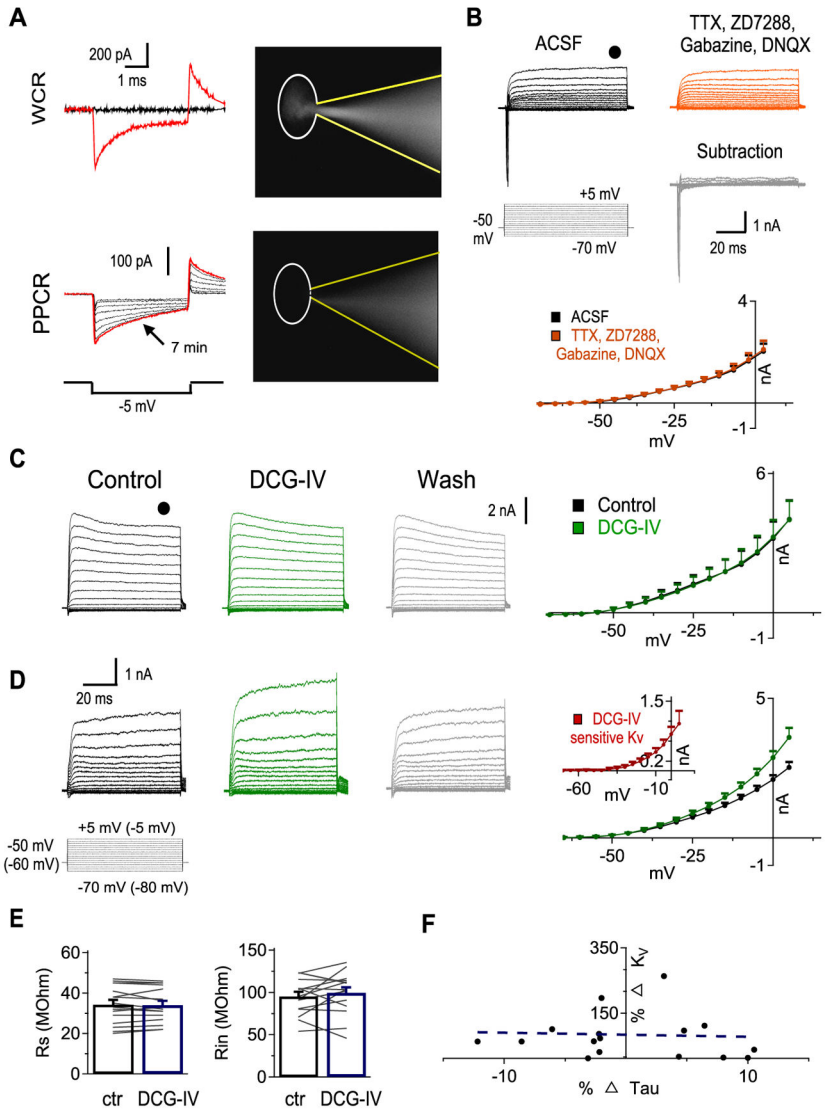

Figure 1.

Perforated patch clamp recordings (PPCR) but not conventional whole-cell recordings (WCR) uncover K_V modulation by mGluR II. ***A***, *top:* Sample cell that spontaneously ruptured into WCR configuration. Note the sudden increase in the test pulse response (red trace) and filling of the cell with a fluorescent dye Lucifer Yellow. *bottom:* Sample cell that had perforated and maintained stable perforation configuration. Note the gradual increase in the test pulse response (the red trace was obtained 7 mins after formation of a tight seal) and absence of Lucifer Yellow inside the cell. The other traces were obtained at about 0, 0.5, 2.5, 3.5, 4.5, 5, and 5.5 mins. The soma of the recorded cell is delineated. ***B,*** Voltage clamp recordings before (black) and after (red) bath application of a cocktail of blockers to isolate K_V currents revealed that stable PPCR was attainable. The subtraction trace (grey) and current-voltage (IV) curves show no changes in steady state K_V currents (n = 8). ***C***, Sample conventional WCR of K_V currents using the protocol shown on the left (V_{hold} = −50 mV, $V_{command}$ = −70 to +5 mV for PPCR and −80 to −5 mV for WCR, 100 ms duration). Steady

state IV curves before (black) and after mGluR II agonist DCG-IV (2 μM, green) application were not different (n = 8). ***D***, Sample PPCR of K_V currents before, during, and after DCG-IV (2 μM) application. IV curves show that DCG-IV increased K_V currents. *inset*: IV curve of DCG IV-sensitive K_V currents (n = 16). ***E***, DCG-IV application did not change series resistance (R_S) or input resistance (R_{in}) of perforated NL neurons (n = 16). ***F,*** The percent change in membrane time constant (τ_M) is not correlated to the percent increase in K_V currents (n = 16, r = 0.047, $p = 0.862$). All the data in the rest of the study were obtained with PPCR. In this and subsequent figures, Means ± SEM are shown. *, **, and *** indicate $p < 0.05$, $p < 0.01$, and $p < 0.001$, respectively.

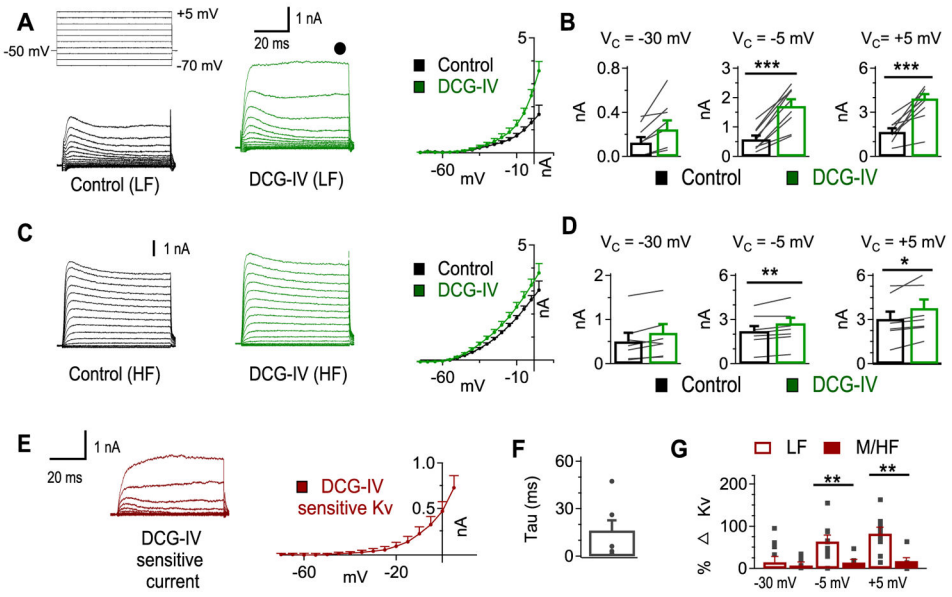

Figure 2.

mGluR II enhancement of K_V currents is most prominent in LF neurons. ***A***, DCG-IV (2 μM) increased K_V currents in LF neurons (n = 9). ***B***, The predominant change in K_V currents was observed at voltage commands more positive than −20 mV, indicating a high threshold K_V (HTK) current was affected by DCG-IV. ***C***, DCG-IV produced a slight increase in K_V currents in MF and HF neurons (n = 7). *D*, The change in K_V currents in MF and HF NL neurons was significantly increased at $V_{command}$ of −5 and +5 mV but not at −30 mV. ***E***, The DCG-IV-sensitive current (DCG-IV K_V currents minus control K_V currents) has noticeable activation at about −20 mV, further confirming it is the HTK component. ***F***, Activation **τ** at $V_{command}$ of −5 mV reveals the DCG-IV-sensitive current is relatively slow (16.3 ± 6.3 ms, n = 7), indicating it is a delayed rectifying current. ***G***, Percent change in K_V was significantly larger for LF (open bars) compared to MF/HF (filled bars) neurons at $V_{command}$ of −5 and +5 mV but not at −30 mV.

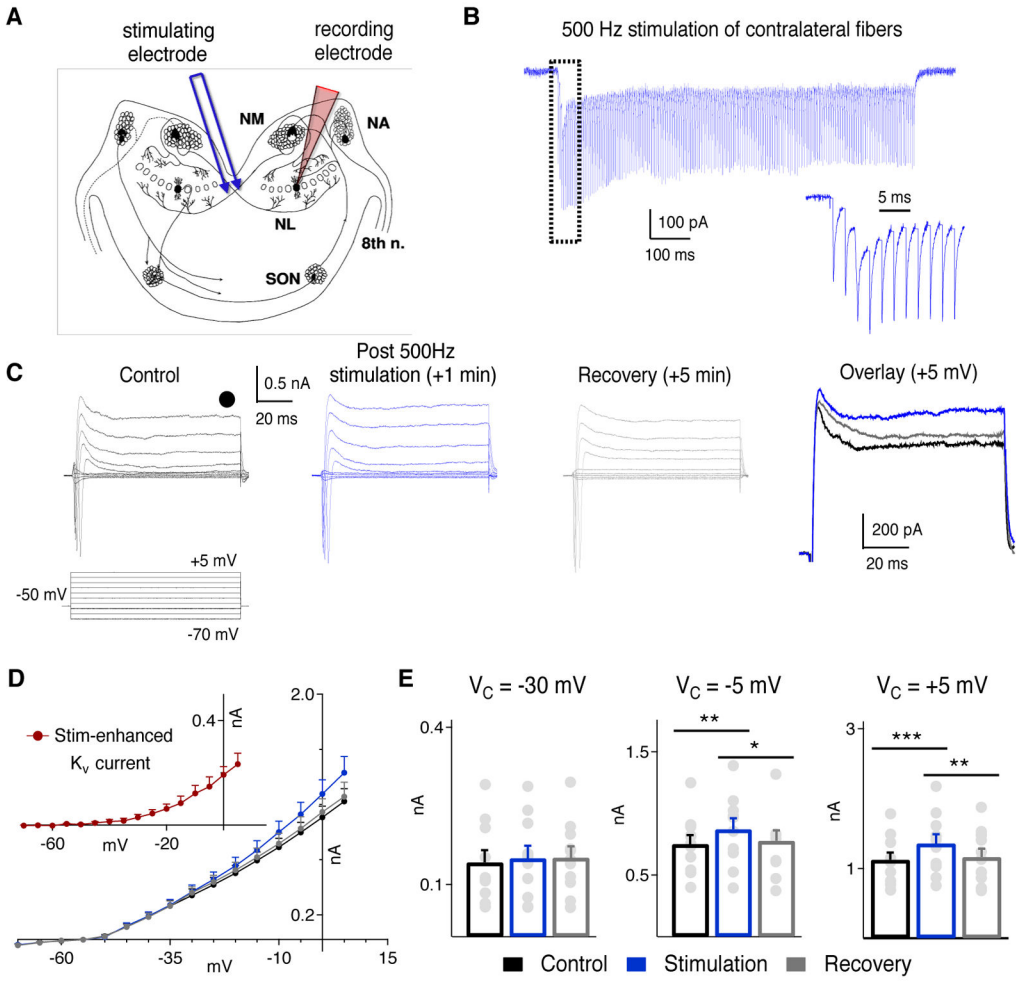

Figure 3.

Endogenous glutamate enhances K_V currents in NL neurons. ***A,*** Schematic showing the auditory circuit in the chicken brainstem, and the placement of the stimulating and recording electrodes. NA: nucleus angularis; NM: nucleus magnocellularis; SON: superior olivary nucleus. ***B,*** Sample voltage clamp recording (V_{hold} = −50 mV) of EPSCs in response to train stimulation (500 Hz, 500 pulses), with the response to the first 11 pulses shown at an enlarged time scale. ***C,*** Sample recording from a neuron before (*black*), immediately after (*blue*), and 5 mins (*grey*) after 5 repetitions of the train stimulation (10 s inter-stimulation interval). An overlay of the currents at $V_{command}$ of +5 mV is shown on the right. ***D,*** IV curves show an increase in the steady state K_V currents immediately after the stimulation, and recovery to baseline levels in 5 mins (n = 10). *Inset*: The stimulation-enhanced K_V current, obtained by subtracting the baseline recordings (black) from the post-stimulation recordings (blue). ***E,*** There was a significant increase in the steady state K_V currents immediately after the stimulation at −5 mV and +5 mV, and the currents returned to the baseline level 5 min after the stimulation was terminated.

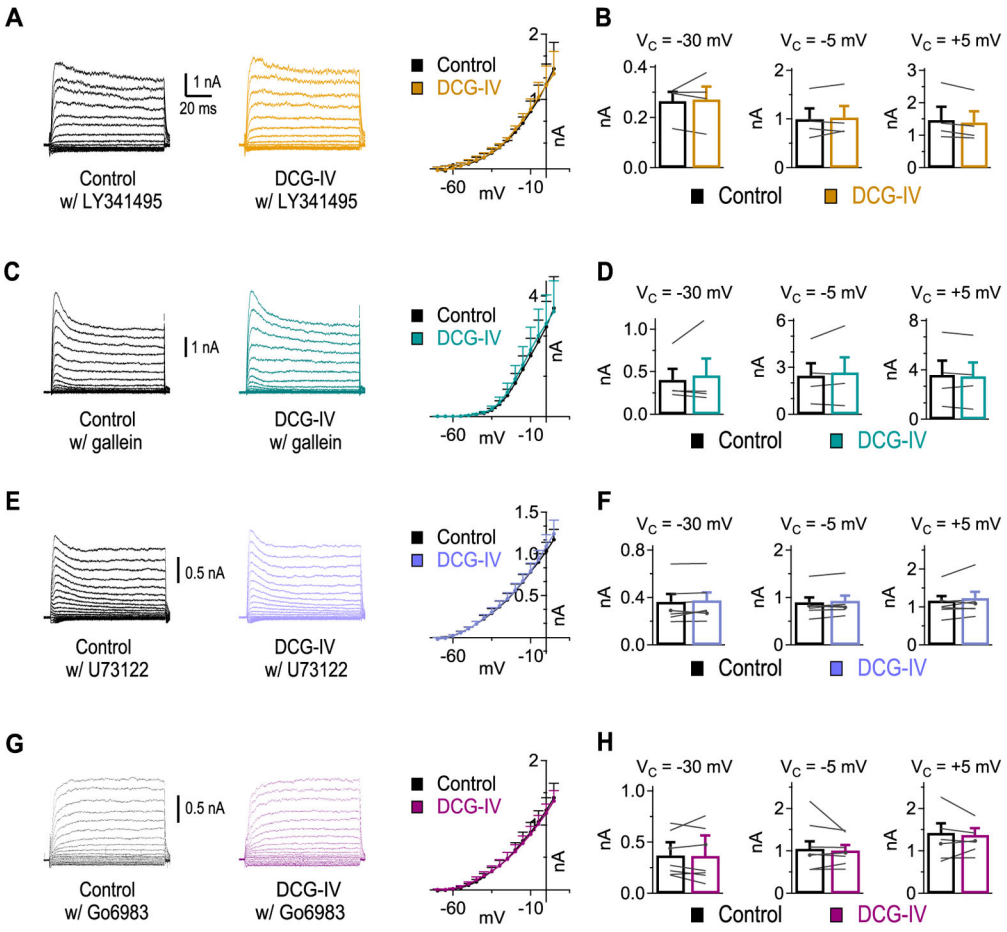

Figure 4.

mGluR II enhancement of K_V currents is dependent on $G_{\beta\gamma}$, phosopholipase C (PLC), and protein kinase C (PKC). ***A***, mGluR II antagonist LY341495 (1 μM) blocked DCG-IV enhancement of K_V currents (n = 4). ***B***, No change in K_V currents was observed at $V_{command}$ of −30, −5, and +5mV in the presence of LY341495. ***C, D,*** Blockade of $G_{\beta\gamma}$ subunits using gallein (5 μM) prevented DCG-IV enhancement of K_V currents (n = 4). ***E, F,*** Cell permeable PLC blocker U73122 (10 μM) eliminated DCG-IV enhancement of K_V currents (n = 7). ***G, H***, Blockade of PKC using Go6983 (20 nM) prevented the DCG-IV enhancement of K_V currents (n = 7).

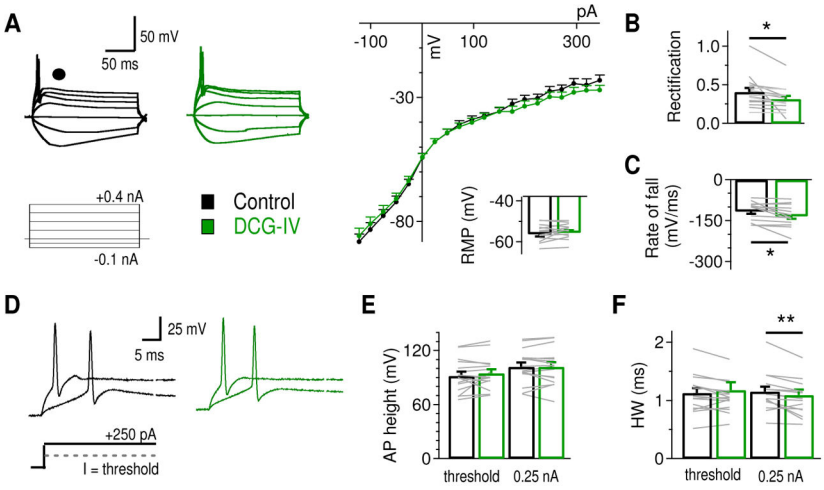

Figure 5.

Effects of mGluR II activation on the intrinsic properties of LF NL neurons. ***A***, Sample membrane potential recordings using a protocol with prolonged somatic current injections (200 ms pulse duration, $I_{injection}$ = −0.1 to +0.4 nA). The voltage-current (V/I) curves show that DCG-IV reduced membrane potentials to the most positive current injections (n = 16). No change in RMP was observed (ctr: −56.2 ± 1.2 mV, DCG-IV: −55.5 ± 1.1 mV). ***B***, DCG-IV significantly reduced the rectification index (the ratio of the slope of voltage deflections to depolarized current injections divided by the slope of voltage deflections to hyperpolarized current injections). ***C***, The absolute AP rate of fall was significantly increased after DCG-IV application. ***D***, Sample APs at threshold and at I = 0.25 nA. ***E***, No significant change in AP height was observed after DCG-IV application. ***F***, DCG-IV reduced AP half-width significantly at I = 0.25 nA (n = 16).

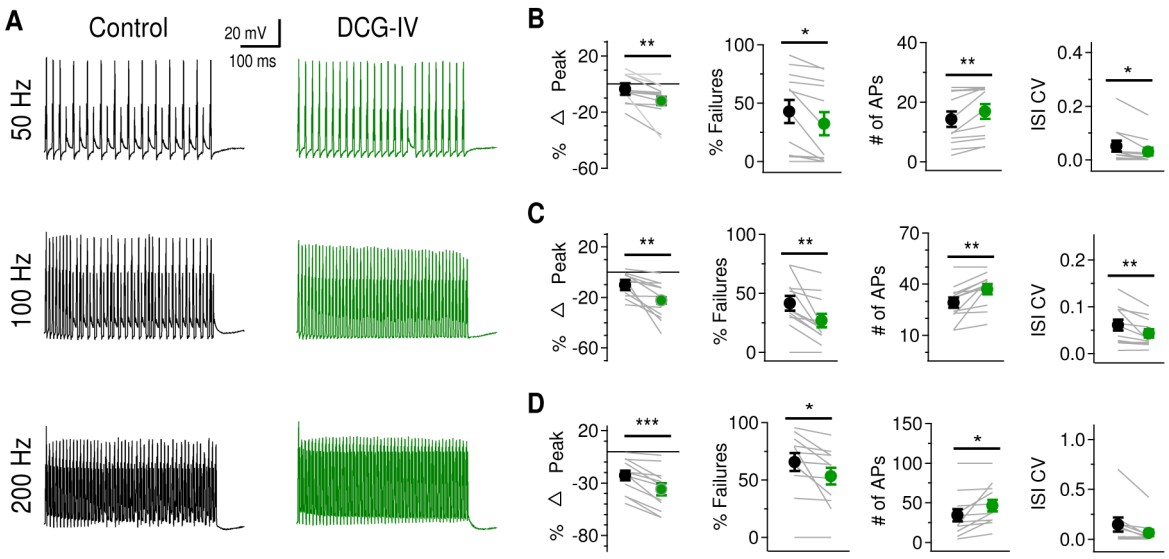

Figure 6.

Activation of mGluR II enhances ability of LF NL neurons to follow high frequency inputs. ***A***, Sample membrane potential recordings in response to current injections (2 ms pulse duration, 500 ms train duration) at 50 Hz (25 pulses), 100 Hz (50 pulses), and 200 Hz (100 pulses) before and after DCG-IV application. ***B***, *left:* At 50 Hz, significant percent reduction in peak AP amplitude (first versus last AP) was observed after DCG-IV application (n = 12). *Middle left:* There was also a significant reduction in the percentage of failures after DCG-IV application. *Middle right:* The number of APs evoked by train stimulation was increased. *Right:* The coefficient of variation in inter-spike interval (ISI CV) was significantly reduced by DCG-IV. ***C***, At 100 Hz, similar significant changes in peak AP amplitude, percentage of failures, number of APs, and ISI CV were observed. ***D***, At 200 Hz, there was a significant reduction in peak AP amplitude, the percentage of failures, and the number of APs. The ISI CV remained unchanged ($p = 0.057$), possibly due to the relatively large variability in control conditions.